Supplementary Information (SI) for Catalysis Science & Technology.
This journal is © The Royal Society of Chemistry 2026

Support information

Exciton-Mediated Singlet Oxygen Generation by a Donor-Acceptor Hydrogen-Bonded Organic Framework for Selective Photocatalytic Oxidative Coupling of Benzylamines

Jin-Lin Li[a, c], Yao Wang[c], Jia-Jun Yu[c], Ying Zou*[c], Lei Cai*[b]

[a] College of Chemistry and Materials Science, Fujian Normal University, Fuzhou 350007, P. R. China

[b] College of Chemistry and Chemical Engineering, Xinjiang Agricultural University, Urumqi 830052, P. R. China

[c] State Key Laboratory of Structural Chemistry, Fujian Institute of Research on the Structure of Matter, Chinese Academy of Sciences, Fuzhou 350002, P. R. China

Experimental Section

1. Materials

N, *N*-dimethylformamide (DMF, AR), potassium carbonate (K_2CO_3), *N*, *N*-dimethylacetamide (DMA, AR), dimethyl sulfoxide (DMSO, AR), methanol (MeOH, AR), ethanol (EtOH, AR), acetone (AR), tetrahydrofuran (THF), acetic acid (HOAc) and potassium hydroxide (KOH) were obtained from Sinopharm. 4,7-dibromobenzo[c][1,2,5]thiadiazole (1) and methyl 4-(4,4,5,5-tetramethyl-1,3,2-dioxaborolan-2-yl)benzoate (2), 1,3,6,8-tetrakis(4,4,5,5-tetramethyl-1,3,2-dioxaborolan-2-yl)pyrene (4), palladium tetrakis(triphenylphosphine) ($Pd(PPh_3)_4$), and sodium chloride (NaCl) was purchased from Adamas.

2. Synthesis of H_4TBTPy

Synthesis of 4,4′,4″,4‴-(pyrene-1,3,6,8-tetrayl) tetrakis(benzo [c] [1,2,5] thiadiazole-7,4-diyl) tetramethyl benzoate

Under N_2 atmosphere, methyl 4-(4-bromobenzo[c][1,2,5]thiadiazol-7-yl)benzoate (3, 630 mg, 0.55 mmol),1,3,6,8-tetrakis(4,4,5,5-tetramethyl-1,3,2-dioxaborolan-2-yl)pyrene (4, 255 mg, 0.123 mmol), potassium carbonate (253 mg, 1.83 mmol), and tetrakis(triphenylphosphine)palladium(0) ($Pd(PPh_3)_4$, 80 mg, 0.07 mmol) were successively dispersed in a mixed solvent of DMF/H_2O (30 mL/5 mL) under nitrogen, and the resulting mixture was heated to reflux at 120°C and stirred for 24 h with the reaction progress monitored by thin-layer chromatography. After cooling to room temperature, acetone (50 mL) was added to induce precipitation, and the resulting solid was collected by centrifugation, washed repeatedly with ethanol (100 mL), and dried to afford a red solid as the crude product, which was dissolved in deuterated chloroform ($CDCl_3$), filtered to remove insoluble impurities, and characterized by ^{1}H NMR spectroscopy: ^{1}H NMR (400 MHz, $CDCl_3$) δ = 8.45 (s, 2H), 8.23 (d, 8H), 8.11 (d, 8H), 8.04–7.95 (m, 12H), 3.97 (s, 12H).

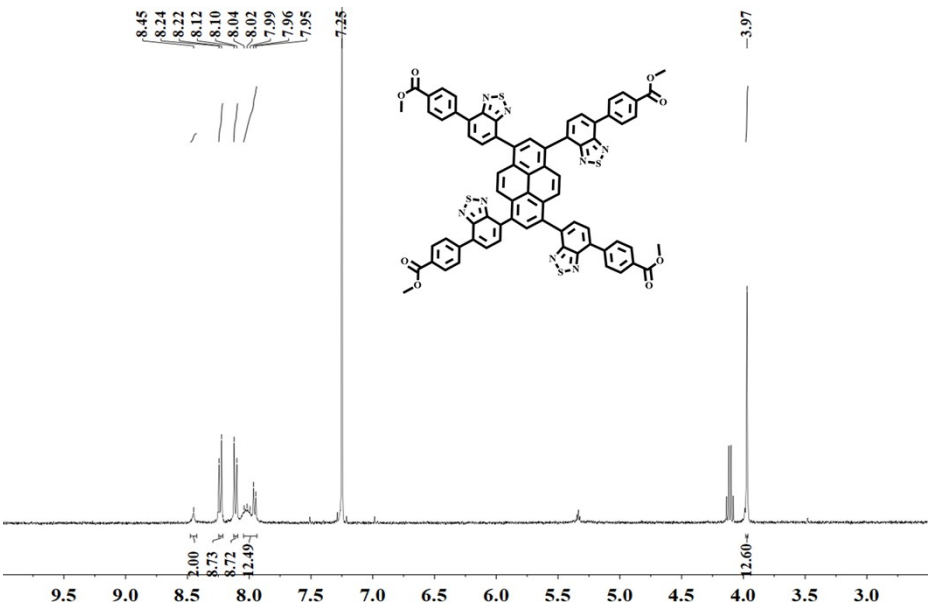

Figure S1 ^{1}H-NMR Spectrum of 4,4',4",4"'-[1,3,6,8-Tetrakis (benzo[c][1,2,5] thiadiazol-7,4-diyl)]pyrene-4,4',4",4"'-tetrakis (benzoic acid) methyl ester.

Synthesis of 4,4′,4″,4‴-(pyrene-1,3,6,8-tetrayl) tetrakis(benzo[c][1,2,5] thiadiazole-7,4-diyl) benzoic acid (H_4TBTPy)

The crude product 4,4′,4″,4‴-(pyrene-1,3,6,8-tetrayl) tetrakis(benzo[c][1,2,5] thiadiazole-7,4-diyl) tetramethyl benzoate (5) was treated with potassium hydroxide (1.5 g) in a mixed solvent of methanol/water/tetrahydrofuran (100 mL, v/v/v = 1:1:8). The reaction mixture was heated to reflux at 85°C for 12 h, with the reaction progress monitored by thin-layer chromatography (TLC). After completion, insoluble impurities were removed by membrane filtration, and the solvents were removed by rotary evaporation. The residue was dissolved in deionized water to afford a clear solution, which was acidified by slow addition of dilute aqueous HCl to pH 1-2 under stirring and allowed to stand overnight. The resulting precipitate was collected by centrifugation, washed three times with dilute HCl (pH = 1), and dried to afford 4,4′,4″,4‴-(pyrene-1,3,6,8-tetrayl)tetrakis(benzo[c][1,2,5]thiadiazole-7,4-diyl)benzoic acid as a red solid.^{1}H NMR (DMSO-d_6): δ = 13.14 (s, 4H), 8.46 (s, 2H), 8.21–8.13 (m, 24H), 8.11 (s, 4H). HR-MS (ESI): m/z calcd for $C_{68}H_{32}N_8O_8S_4^-$ [M-2H]$^-$: 1216.0636, found: 1218.159.

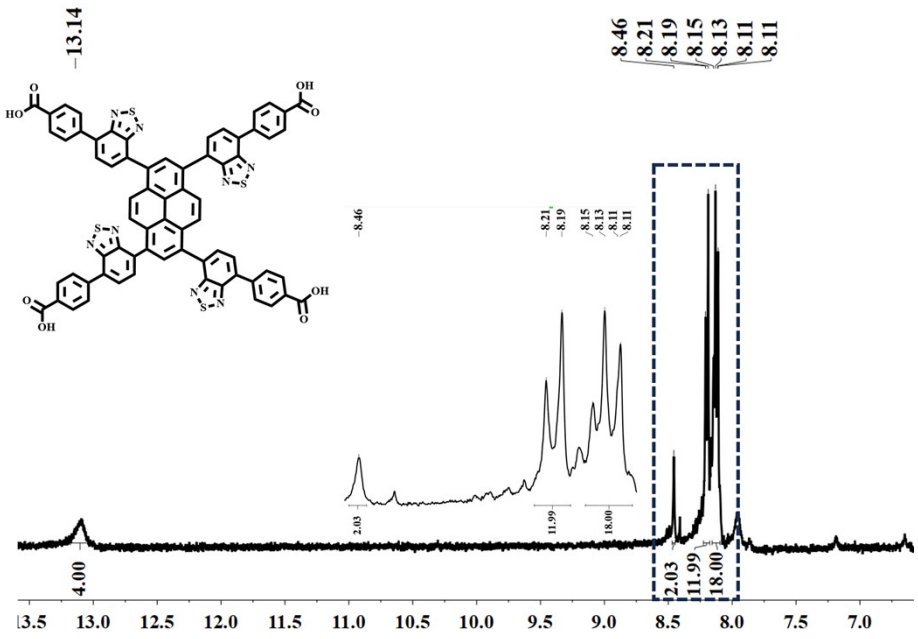

Figure S2 ^{1}H NMR Spectrum of H_4TBTPy.

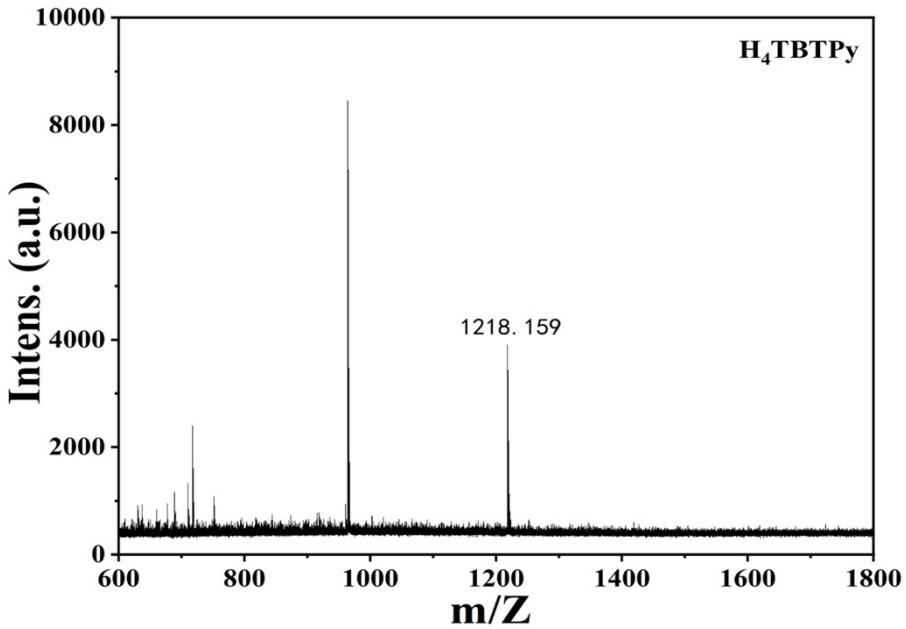

Figure S3 Mass spectrum of H_4TBTPy.

3. Synthesis of PFC-111

H_4TBTPy (20 mg, 0.015 mmol) was dissolved in *N*, *N*-dimethylacetamide (DMA, 2.0 mL) under ultrasonication until a homogeneous solution was obtained. Methanol (10.0 mL) was then added dropwise with gentle stirring. The resulting mixture was kept at room temperature for 12 h, during which a red precipitate formed. The solid was

isolated by centrifugation (12000 rpm), washed with acetone (2 × 10 mL), and dried in a vacuum oven at 80°C for 10 h to afford PFC-111 as a red powder (15 mg, 75% yield).

4. Photocatalysis Experiment Procedure

Photocatalytic experiments were conducted in a WP-TEC-1020LC parallel photoreactor. In a typical procedure, PFC-111 (5 mg) was dispersed in ethyl acetate (2 mL) by ultrasonication, followed by addition of benzylamine (0.20 mmol). The resulting suspension was stirred under an O_2 atmosphere and irradiated with a 465–470 nm LED while the reaction temperature was maintained at 25 °C using a thermostatic bath. After completion of the reaction, the catalyst was separated by centrifugation and washed repeatedly with ethyl acetate, while the combined organic phases were analyzed by quantitative ^{1}HNMR spectroscopy using CH_2Br_2 (0.10 mmol) as the internal standard (Figure S7).

5. N_2 sorption Isotherms and Pore Size Distribution

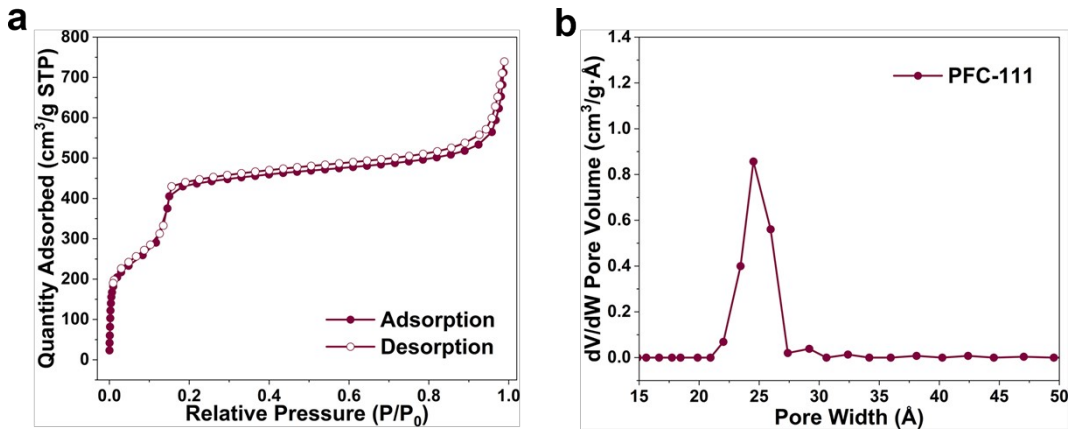

Figure S4 N_2 sorption Isotherm and Pore Size Distribution of PFC-111.

6. Chemical Stability

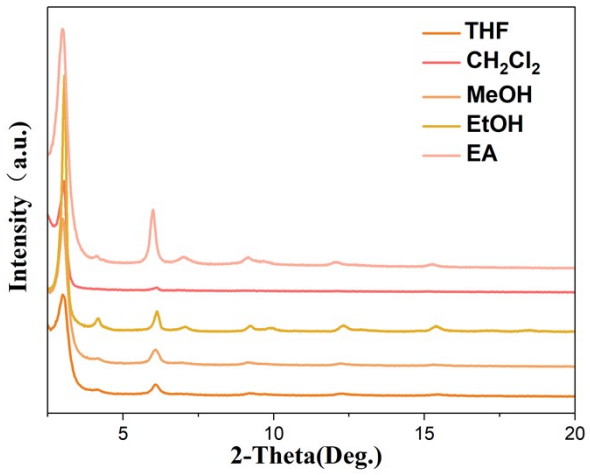

Figure S5 PXRD patterns of PFC-111 soaked in various solvents.

7. TGA Curves

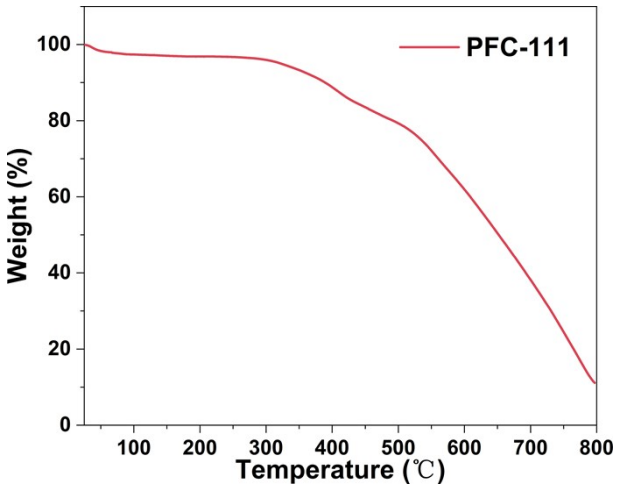

Figure S6 TGA curves of activated PFC-111.

8. Photocatalytic experiment

Photocatalytic experiments were conducted in a WP-TEC-1020LC parallel photoreactor. In a typical procedure, PFC-111 (5 mg) was dispersed in ethyl acetate (2 mL) by ultrasonication, followed by addition of benzylamine (0.20 mmol). The resulting suspension was stirred at 25°C under an O_2 atmosphere and irradiated with a 465-470 nm LED (10 W) for 1 h. After completion of the reaction, the catalyst was separated by centrifugation and washed repeatedly with ethyl acetate, while the combined organic phases were analyzed by quantitative ^{1}H NMR spectroscopy using CH_2Br_2 (0.10 mmol) as the internal standard.

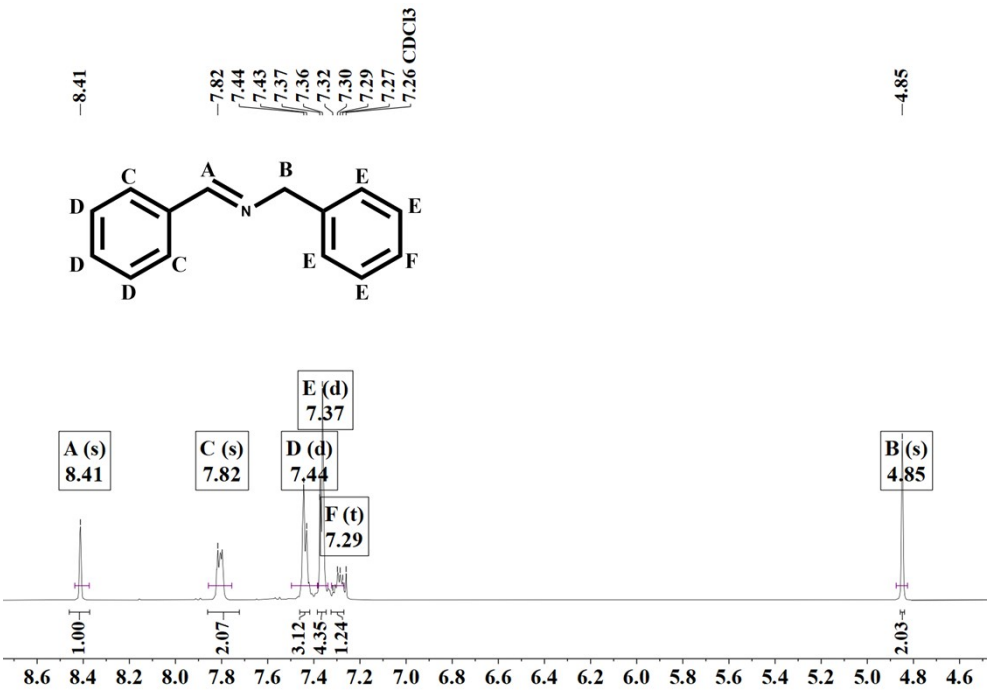

Figure S7 ^{1}H NMR spectrum of imine products.

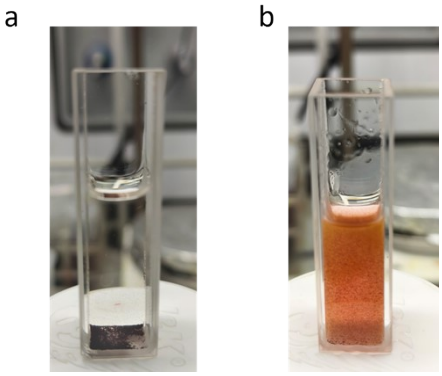

Figure S8 Dispersibility under catalytic conditions in ethyl acetate: (a) H_4TBTPy; (b) PFC-111.

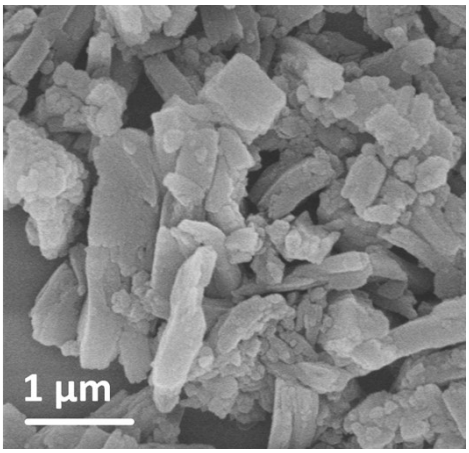

Figure S9 SEM image of PFC-111 after catalysis.

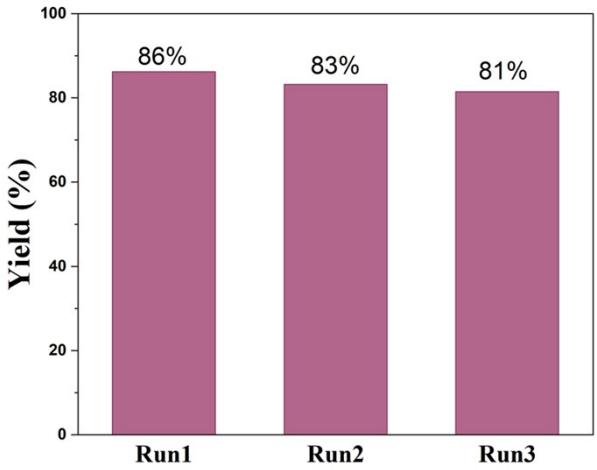

Figure S10 Photocatalytic cycling experiment of PFC-111.

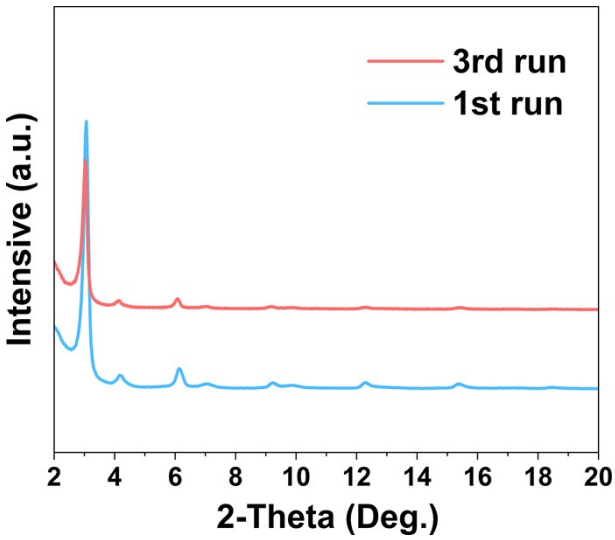

Figure S11 PXRD data after one cycle and three cycles.

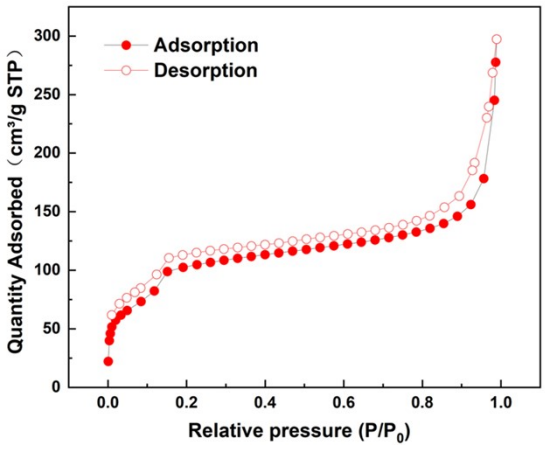

Figure S12 N_2 sorption Isotherm of PFC-111 after three catalytic cycles.

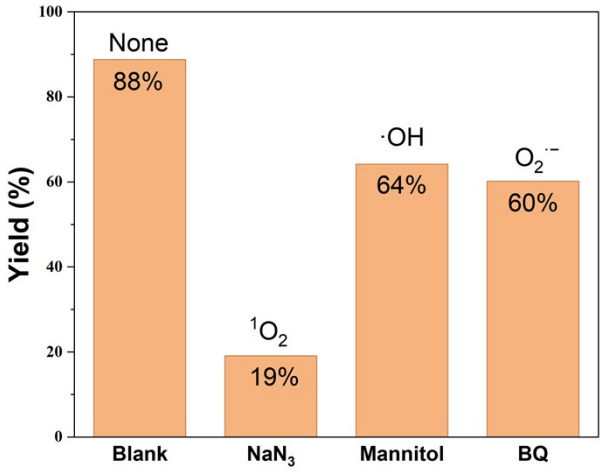

Figure S13 Active oxygen scavenging experiment for PFC-111.

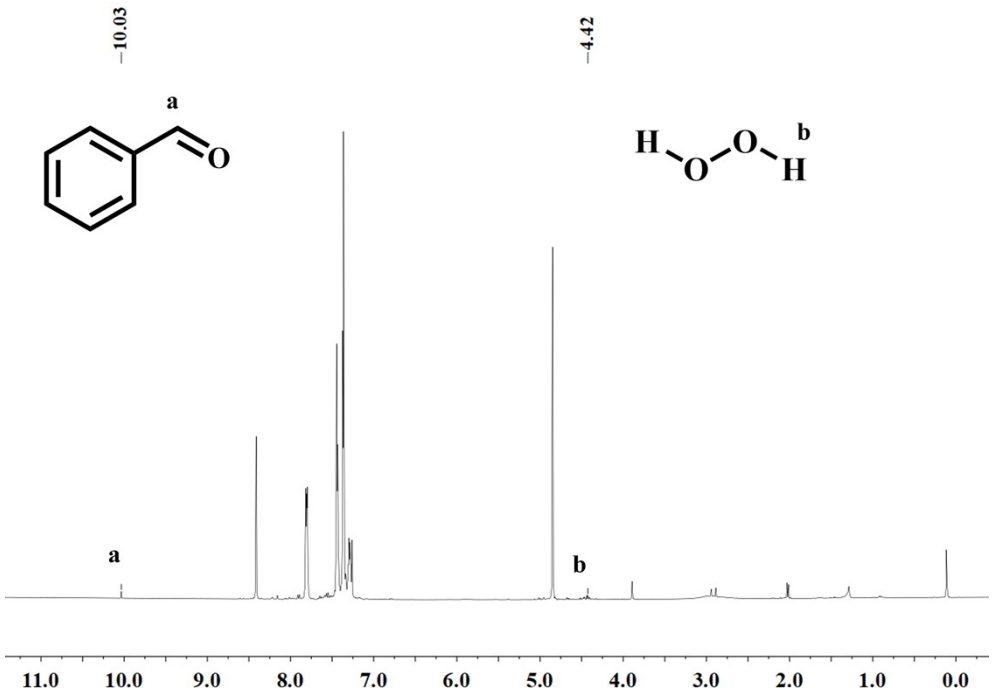

Figure S14 ^{1}H NMR spectrum of Benzaldehyde.

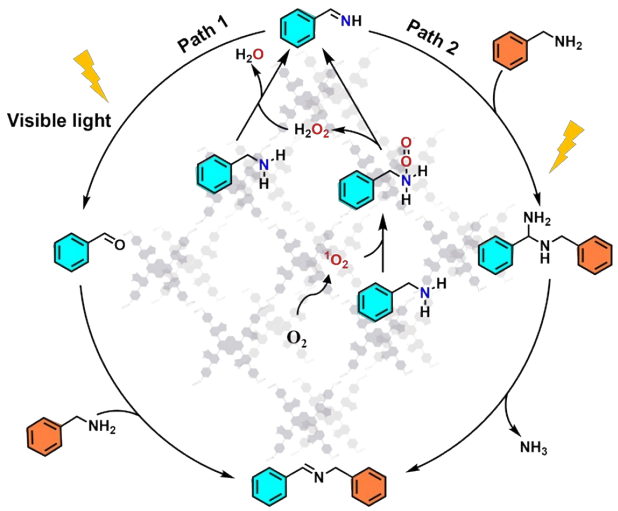

Figure. S15 The proposed reaction mechanism.

9. Density Functional Theory (DFT) calculation

To reveal the catalytic sites for converting oxygen to singlet oxygen. The Bader charges of the atoms in the H_4TBTPy (the building unit of PFC-111) and the Gibbs free energy required for oxygen activation at different sites on H_4TBTPy were calculated by density functional theory (DFT) through Vienna Ab initio Simulation Package (VASP)[1-4]. The Projector Augmented Wave (PAW)[5-6] in conjunct with the Perdew-Burke-Ernzerhof (PBE) flavor[7] were carried out in all calculations. The k-point sampling of (2,2,1) for H_4TBTPy were employed. The convergence criteria and the cutoff energy of plane wave basis was set to 1×10^{-4} eV and 400 eV, respectively. The threshold for force was set to -0.1 eV·Å^{-1}, and the Van der Waals (vdW) correction was adopted by Grimme (DFT+D3)[8]. To avoid the periodic interactions of the system, a vacuum region of 15 Å between two repeated slabs was used in the direction perpendicular to the surface. Over these optimized structures, vibration frequencies were calculated to obtain zero-point energies, and entropy contributions, and the convergence criteria was set to 1×10^{-5} eV. When calculating the vibration frequencies, only the adsorbate was allowed to relax. The ΔG_0 was calculated at 298.15 K by the VASPKIT package[9], which according to $\Delta G_0 = \Delta E_{DFT} + \Delta E_{ZPE} - T\Delta S$. The E_{DFT}, E_{ZPE} and S indicates the electronic energy, zero-point energy and entropy, respectively.

10. ^{1}H NMR spectra of imine products

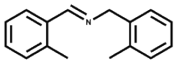

^{1}H NMR (400 MHz, Chloroform-*d*) δ 8.68 (s, 1H), 7.94 (d, *J* = 9.0 Hz, 1H), 7.31 (dd, *J* = 7.4, 1.6 Hz, 2H), 7.26 (d, *J* = 6.7 Hz, 1H), 7.20 (d, *J* = 2.8 Hz, 4H), 4.84 (s,2H), 2.52 (s, 3H), 2.40 (s, 3H).

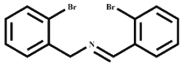

^{1}H NMR (400 MHz, Chloroform-*d*) δ 8.81 (s, 1H), 8.11 (d, *J* = 7.7 Hz, 1H), 7.58 (d, *J* = 7.9 Hz, 2H), 7.42 (d, *J* = 7.6 Hz, 1H), 7.37 – 7.27 (m, 3H), 7.18 – 7.12 (m, 1H), 4.93 (s, 2H).

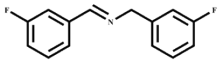

^{1}H NMR (400 MHz, Chloroform-*d*) δ 8.37 (s, 1H), 7.59 – 7.47 (m, 2H), 7.39 (q, *J* = 8.1, 7.5 Hz, 1H), 7.31 (q, *J* = 8.0, 7.2 Hz, 1H), 7.18 – 7.09 (m, 2H), 7.06 (d, *J* = 9.8 Hz, 1H), 6.96 (t, *J* = 8.4 Hz, 1H), 4.81 (s, 2H).

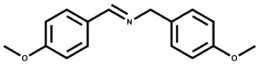

^{1}H NMR (400 MHz, Chloroform-*d*) δ 8.30 (s, 1H), 7.72 (d, *J* = 8.8 Hz, 2H), 7.25 (d, *J* = 8.5 Hz, 2H), 6.90 (dd, *J* = 16.6, 8.7 Hz,4H), 4.73 (s, 2H), 3.84 (s, 3H), 3.80 (s, 3H).

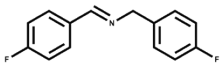

^{1}H NMR (400 MHz, Chloroform-*d*) δ 8.33 (s, 1H), 7.76 (dt, *J* = 8.1, 4.0 Hz, 2H), 7.28 (dd, *J* = 8.1, 5.6 Hz, 2H), 7.07 (dd, *J* = 18.1, 9.8 Hz, 2H), 4.75 (s, 2H).

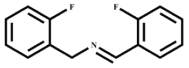

^{1}H NMR (400 MHz, Chloroform-*d*) δ 8.73 (s, 1H), 8.03 (td, *J* = 7.6, 1.8 Hz, 1H), 7.39 (q, *J* = 7.3, 6.8 Hz, 2H), 7.28-7.25 (m, 1H), 7.19 – 7.05 (m, 4H), 4.88 (s,2H).

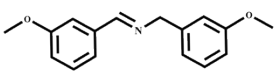

^{1}H NMR (400 MHz, Chloroform-*d*) δ 8.37 (s, 1H), 7.43 – 7.38 (m, 1H), 7.37 – 7.27 (m, 3H), 7.00 (ddd, *J* = 7.7, 2.5, 1.7 Hz, 1H), 6.97 – 6.90 (m, 2H), 6.83 (dd, *J* = 8.2, 2.4 Hz, 1H), 4.81 (s, 2H), 3.86 (s, 3H), 3.82 (s, 3H).

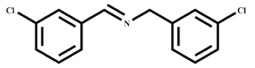

^{1}H NMR (400 MHz, Chloroform-*d*) δ 8.31 (s, 1H), 7.79 (s, 1H), 7.60 (d, *J* = 7.5 Hz, 1H), 7.42 – 7.35 (m, 1H), 7.37 – 7.26 (m, 2H), 7.25 – 7.17 (m, 3H), 4.76 (s, 2H).

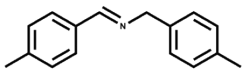

^{1}H NMR (400 MHz, Chloroform-*d*) δ 8.37 (s, 1H), 7.70 (d, *J* = 8.0 Hz, 2H), 7.29 – 7.25 (m, 2H), 7.24 (s, 2H), 7.18 (d, *J* = 7.9 Hz, 2H), 4.80 (s, 2H), 2.41 (s, 3H), 2.37 (s, 3H).

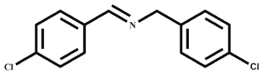

^{1}H NMR (400 MHz, Chloroform-*d*) δ 8.33 (s, 1H), 7.70 (d, *J* = 8.4 Hz, 2H), 7.38 (d, *J* = 8.4 Hz, 2H), 7.30 (d, *J* = 8.5 Hz, 2H), 7.24 (d, *J* = 3.0 Hz, 2H), 4.76 (s, 2H).

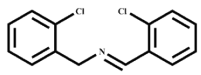

^{1}H NMR (400 MHz, Chloroform-*d*) δ 8.88 (s, 1H), 8.12 (d, *J* = 7.6 Hz, 1H), 7.46 – 7.26 (m, 6H), 7.26 – 7.23 (m, 1H), 4.95 (d, *J* = 1.5 Hz, 2H).

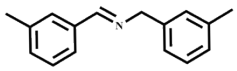

^{1}H NMR (400 MHz, Chloroform-*d*) δ 8.37 (s, 1H), 7.66 (s, 1H), 7.55 (d, *J* = 7.5 Hz, 1H), 7.32 (t, *J* = 7.5 Hz, 1H), 7.23 (d, *J* = 7.4 Hz, 1H), 7.14 (d, *J* = 8.4 Hz, 2H), 7.08 (d, *J* = 7.5 Hz, 1H), 4.79 (s, 2H), 2.39 (s, 3H), 2.36 (s, 3H).

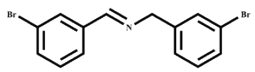

^{1}H NMR (400 MHz, Chloroform-*d*) δ 8.32 (s, 1H), 7.97 (s, 1H), 7.67 (d, *J* = 7.7 Hz, 1H), 7.56 (d, *J* = 8.0 Hz, 1H), 7.48 (s, 1H), 7.40 (d, *J* = 7.7 Hz, 1H), 7.26(m, 3H), 4.78 (s, 2H).

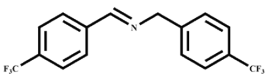

^{1}H NMR (400 MHz, Chloroform-*d*) δ 8.47 (s, 1H), 7.91 (d, *J* = 8.0 Hz, 2H), 7.69 (d, *J* = 8.0 Hz, 2H), 7.61 (d, *J* = 7.9 Hz, 2H), 7.47 (d, *J* = 7.9 Hz, 2H), 4.90 (s, 2H).

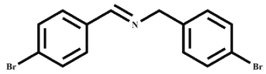

^{1}H NMR (400 MHz, Chloroform-*d*) δ 8.33 (s, 1H), 7.64 (d, *J* = 8.5 Hz, 2H), 7.55 (d, *J* = 8.5 Hz, 2H), 7.47 (d, *J* = 8.4 Hz, 2H), 7.21 (d, *J* = 8.4 Hz, 2H), 4.75 (s, 2H).

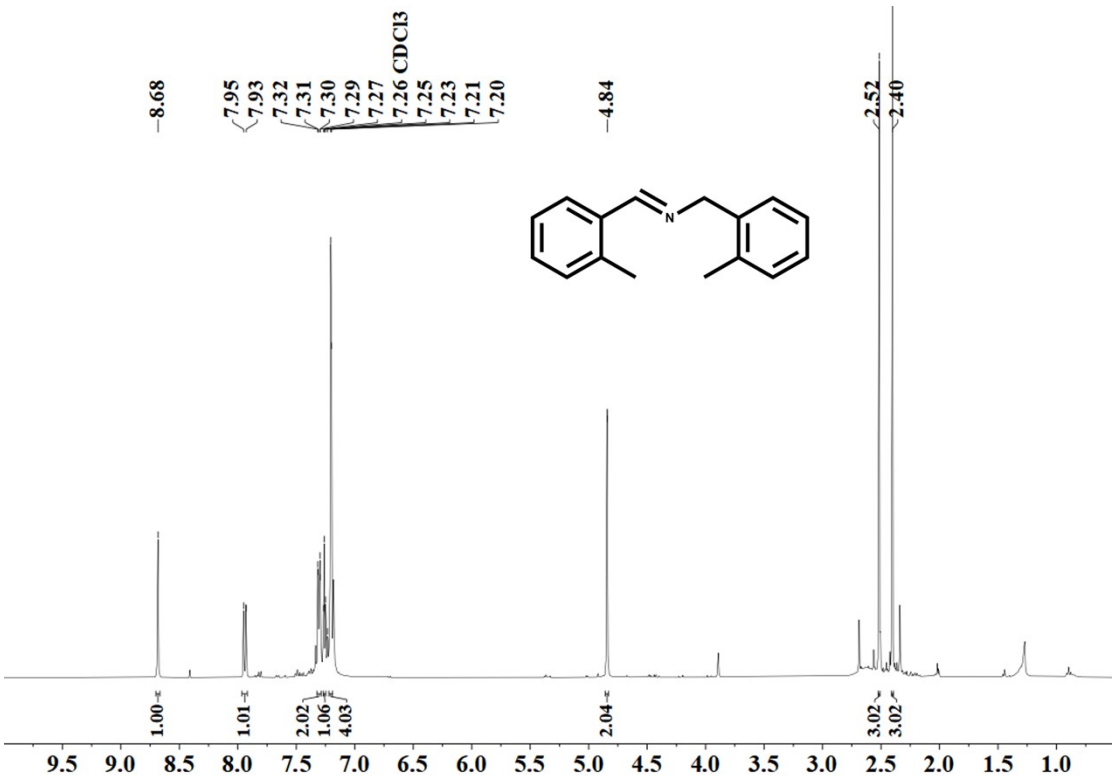
8.68
7.95
7.93
7.32
7.31
7.30
7.29
7.27
7.26 CDCl3
7.25
7.23
7.21
7.20
4.84
2.52
2.40
N
1.00
1.01
2.02
1.06
4.03
2.04
3.02
3.02
9.5 9.0 8.5 8.0 7.5 7.0 6.5 6.0 5.5 5.0 4.5 4.0 3.5 3.0 2.5 2.0 1.5 1.0

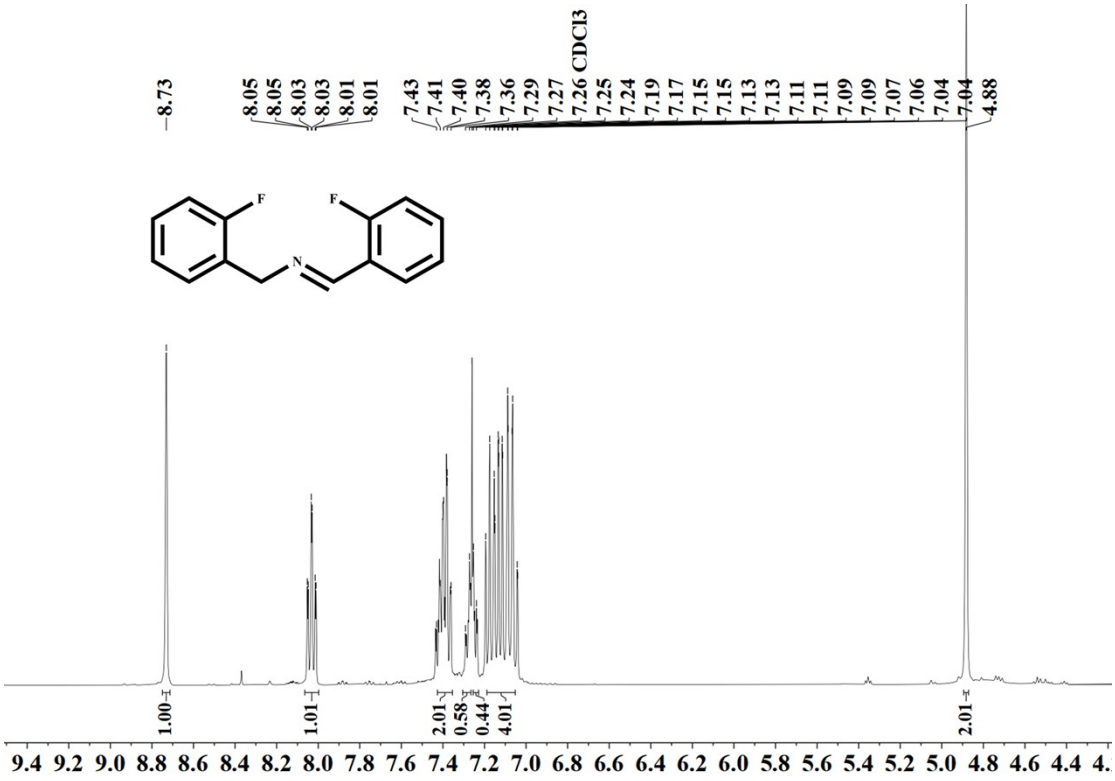
8.73
8.05
8.05
8.03
8.03
8.01
8.01
7.43
7.41
7.40
7.38
7.36
7.29
7.27
7.26 CDCl3
7.25
7.24
7.19
7.17
7.15
7.15
7.13
7.13
7.11
7.11
7.09
7.09
7.07
7.06
7.04
7.04
4.88
F
F
N
1.00
1.01
2.01
0.58
0.44
4.01
2.01
9.4 9.2 9.0 8.8 8.6 8.4 8.2 8.0 7.8 7.6 7.4 7.2 7.0 6.8 6.6 6.4 6.2 6.0 5.8 5.6 5.4 5.2 5.0 4.8 4.6 4.4 4.

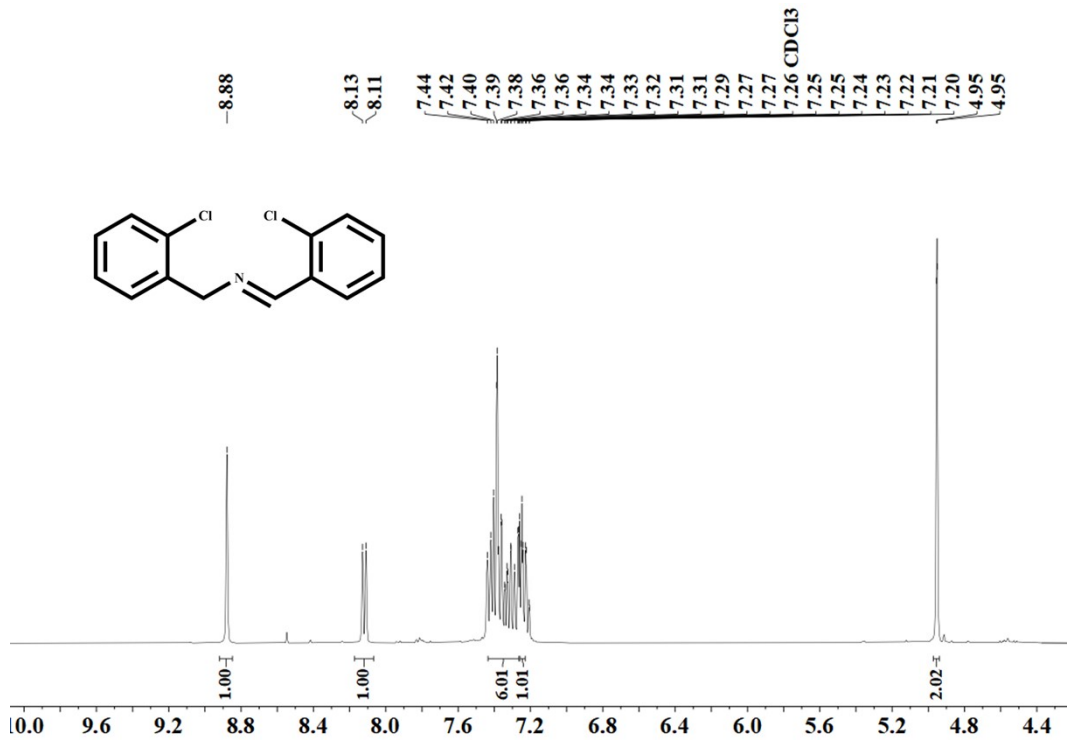
8.88
8.13
8.11
7.44
7.42
7.40
7.39
7.38
7.36
7.36
7.34
7.34
7.33
7.32
7.31
7.31
7.29
7.27
7.27
7.26 CDCl3
7.25
7.25
7.24
7.23
7.22
7.21
7.20
4.95
4.95
Cl
Cl
N
1.00
1.00
6.01
1.01
2.02
10.0
9.6
9.2
8.8
8.4
8.0
7.6
7.2
6.8
6.4
6.0
5.6
5.2
4.8
4.4

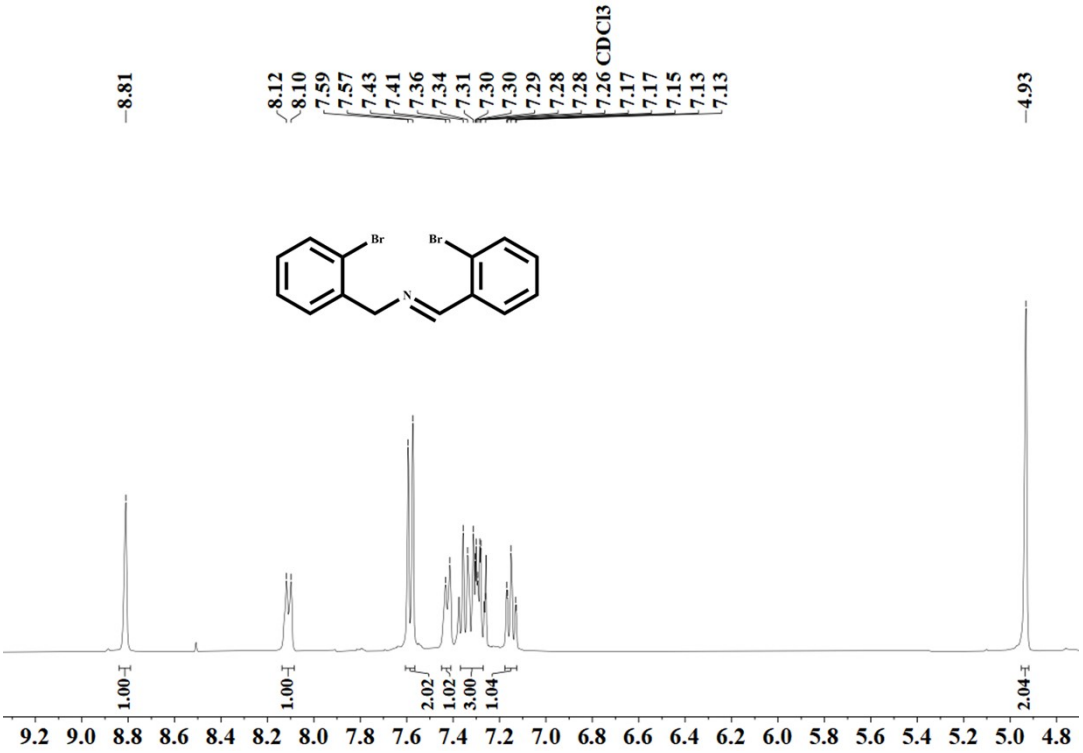
8.81
8.12
8.10
7.59
7.57
7.43
7.41
7.36
7.34
7.31
7.30
7.30
7.29
7.28
7.28
7.26 CDCl3
7.17
7.17
7.15
7.13
7.13
4.93
Br
Br
N
1.00
1.00
2.02
1.02
3.00
1.04
2.04
9.2
9.0
8.8
8.6
8.4
8.2
8.0
7.8
7.6
7.4
7.2
7.0
6.8
6.6
6.4
6.2
6.0
5.8
5.6
5.4
5.2
5.0
4.8

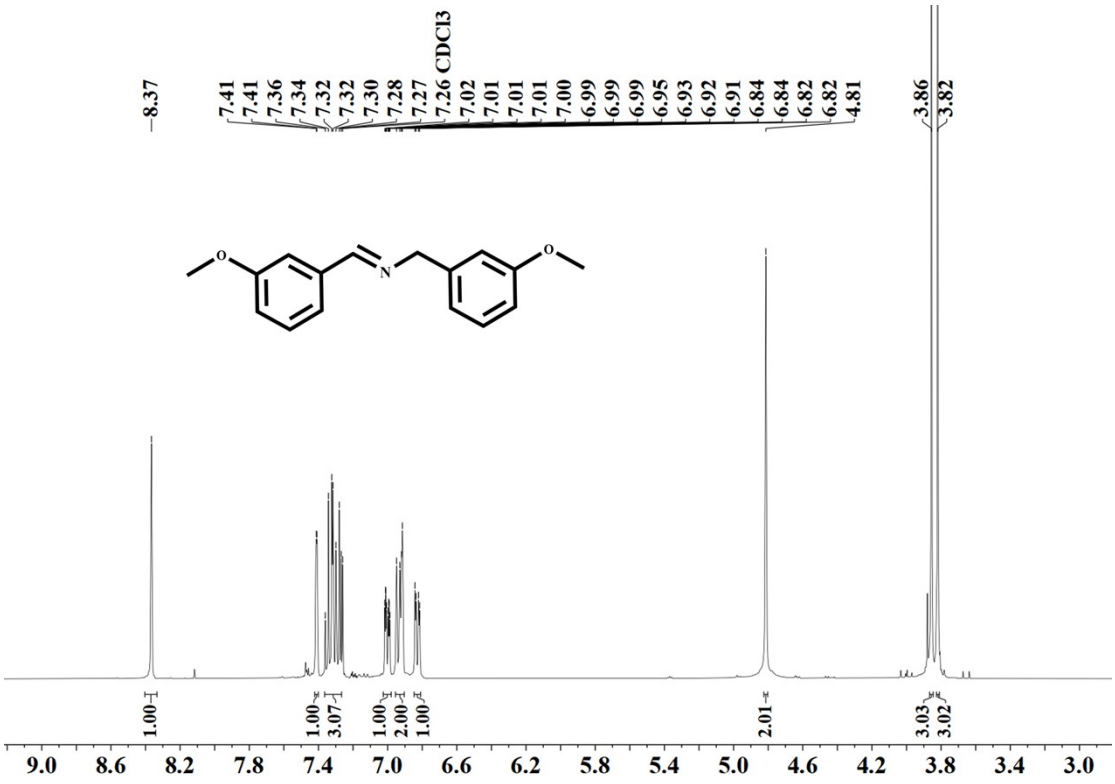
8.37
7.41
7.41
7.36
7.34
7.32
7.32
7.30
7.28
7.27
7.26 CDCl3
7.02
7.01
7.01
7.01
7.00
6.99
6.99
6.99
6.95
6.93
6.92
6.91
6.84
6.84
6.82
6.82
4.81
3.86
3.82
O
N
O
1.00
1.00
3.07
1.00
2.00
1.00
2.01
3.03
3.02
9.0
8.6
8.2
7.8
7.4
7.0
6.6
6.2
5.8
5.4
5.0
4.6
4.2
3.8
3.4
3.0

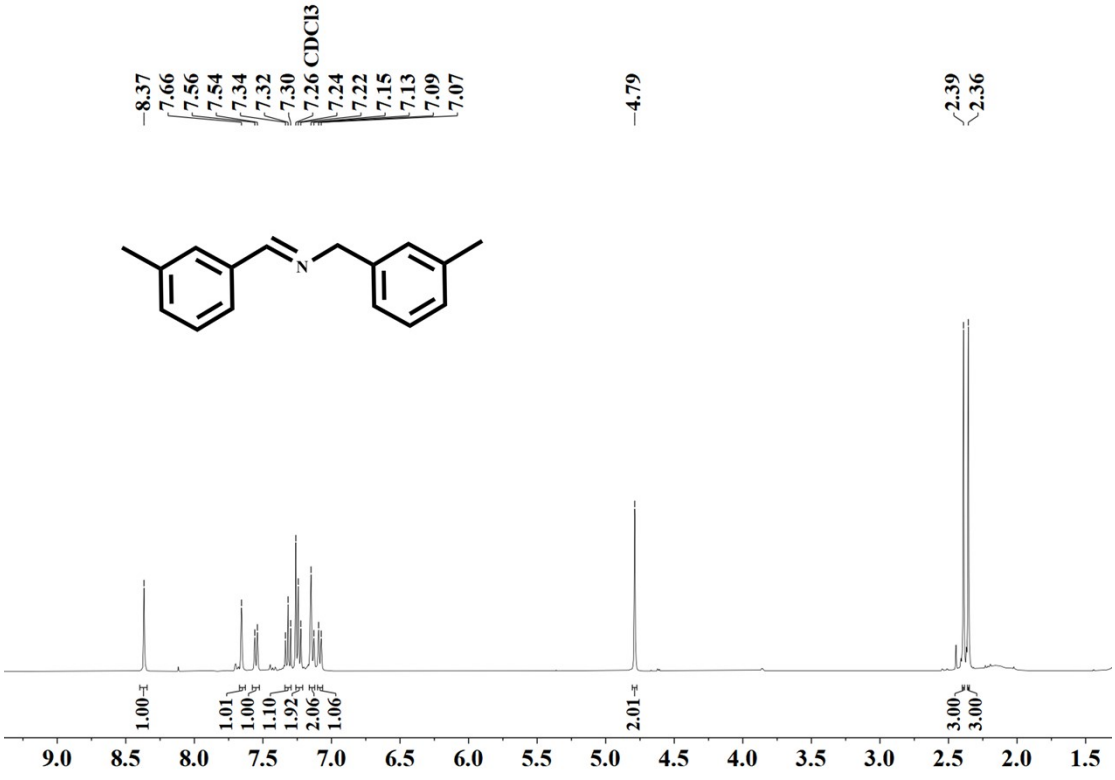
8.37
7.66
7.56
7.54
7.34
7.32
7.30
7.26 CDCl3
7.24
7.22
7.15
7.13
7.09
7.07
4.79
2.39
2.36
N
1.00
1.01
1.00
1.10
1.92
2.06
1.06
2.01
3.00
3.00
9.0
8.5
8.0
7.5
7.0
6.5
6.0
5.5
5.0
4.5
4.0
3.5
3.0
2.5
2.0
1.5

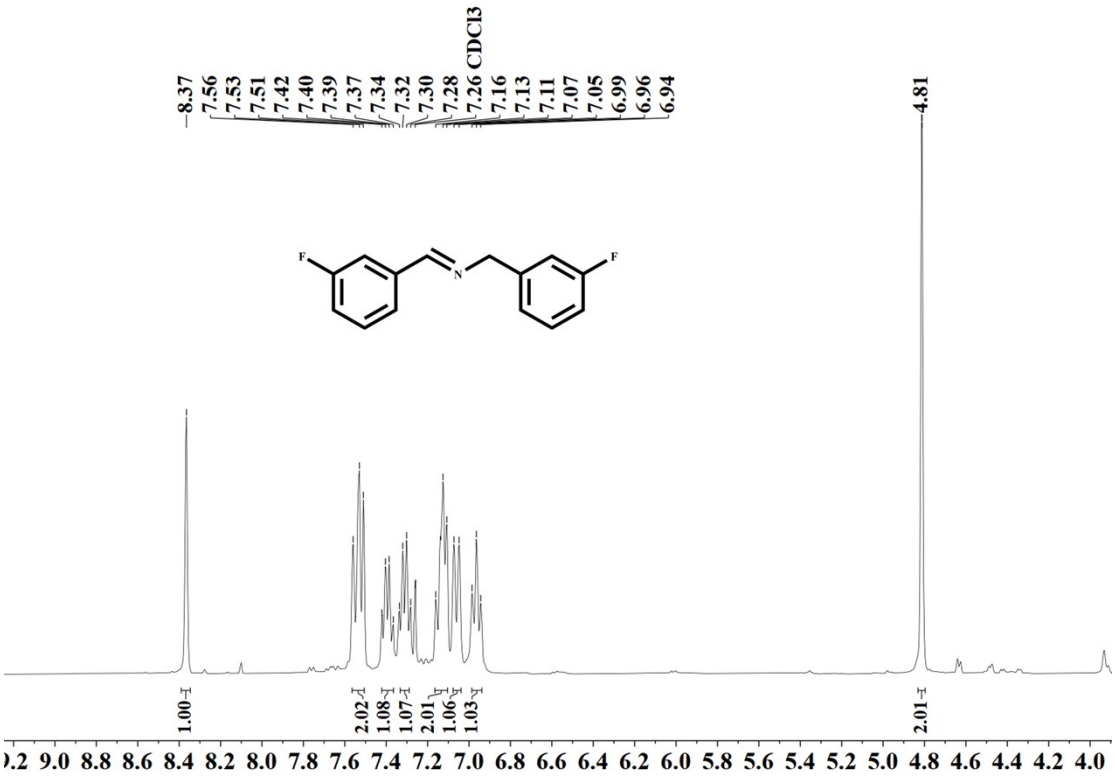
8.37
7.56
7.53
7.51
7.42
7.40
7.39
7.37
7.34
7.32
7.30
7.28
7.26 CDCl3
7.16
7.13
7.11
7.07
7.05
6.99
6.96
6.94
4.81
F
N
F
1.00
2.02
1.08
1.07
2.01
1.06
1.03
2.01
9.2 9.0 8.8 8.6 8.4 8.2 8.0 7.8 7.6 7.4 7.2 7.0 6.8 6.6 6.4 6.2 6.0 5.8 5.6 5.4 5.2 5.0 4.8 4.6 4.4 4.2 4.0

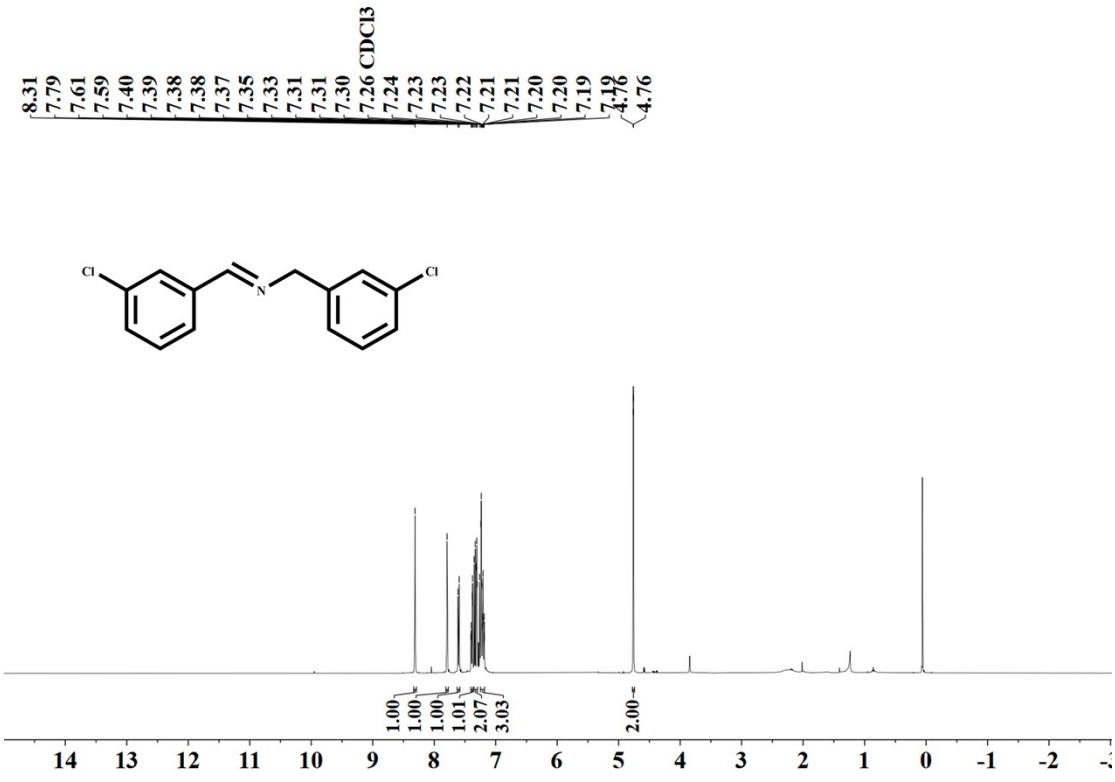
8.31
7.79
7.61
7.59
7.40
7.39
7.38
7.38
7.37
7.35
7.33
7.31
7.31
7.30
7.26 CDCl3
7.24
7.23
7.23
7.22
7.21
7.21
7.20
7.20
7.19
4.76
4.76
Cl
N
Cl
1.00
1.00
1.00
1.01
2.07
3.03
2.00
14 13 12 11 10 9 8 7 6 5 4 3 2 1 0 -1 -2

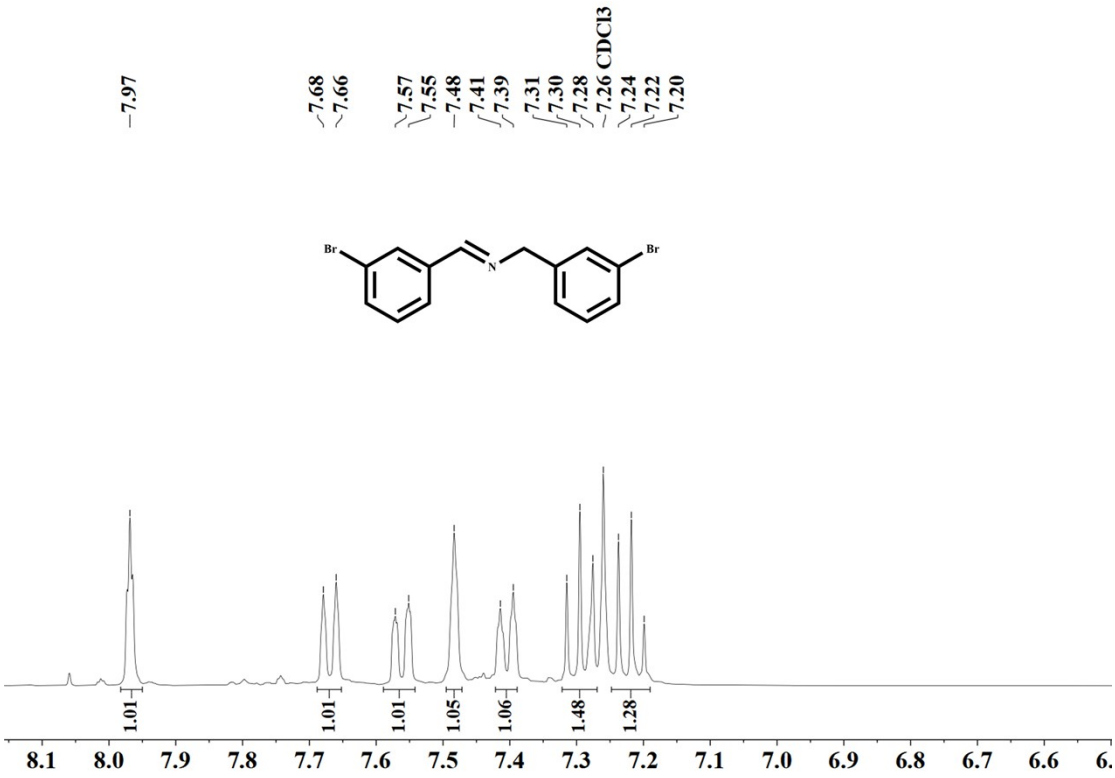
7.97
7.68
7.66
7.57
7.55
7.48
7.41
7.39
7.31
7.30
7.28
7.26 CDCl3
7.24
7.22
7.20
Br
N
Br
1.01
1.01
1.01
1.05
1.06
1.48
1.28
8.1
8.0
7.9
7.8
7.7
7.6
7.5
7.4
7.3
7.2
7.1
7.0
6.9
6.8
6.7
6.6

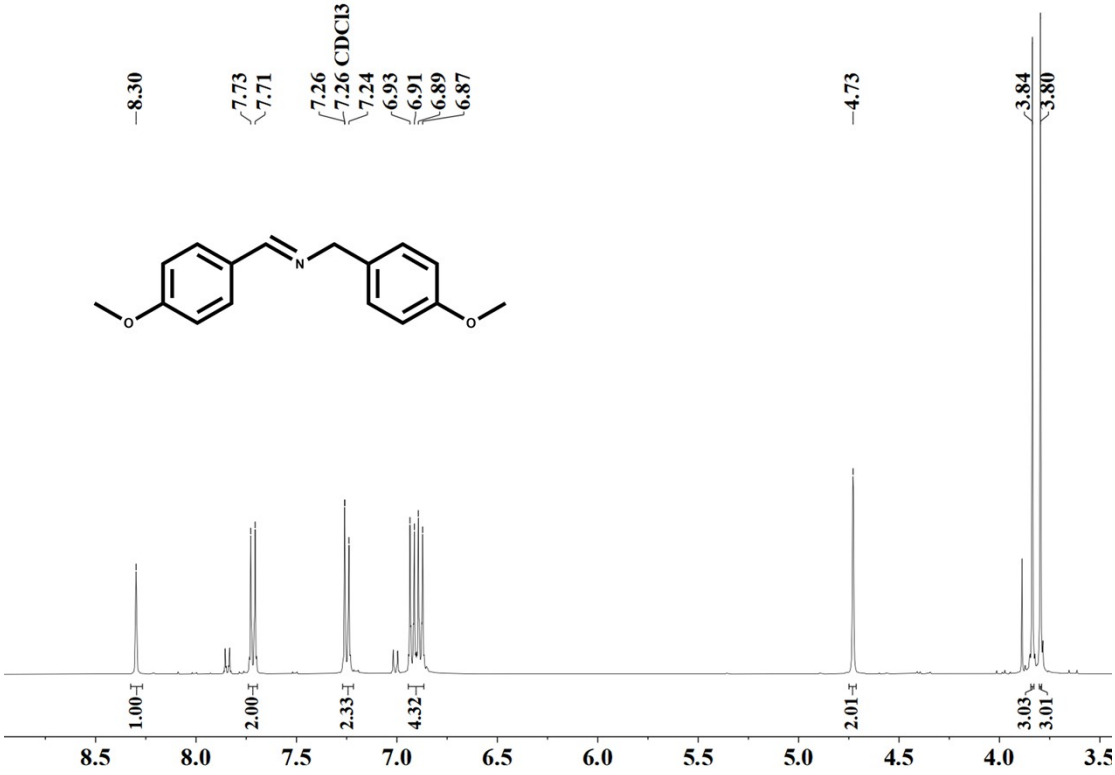
8.30
7.73
7.71
7.26
7.26 CDCl3
7.24
6.93
6.91
6.89
6.87
4.73
3.84
3.80
N
O
O
1.00
2.00
2.33
4.32
2.01
3.03
3.01
8.5
8.0
7.5
7.0
6.5
6.0
5.5
5.0
4.5
4.0
3.5

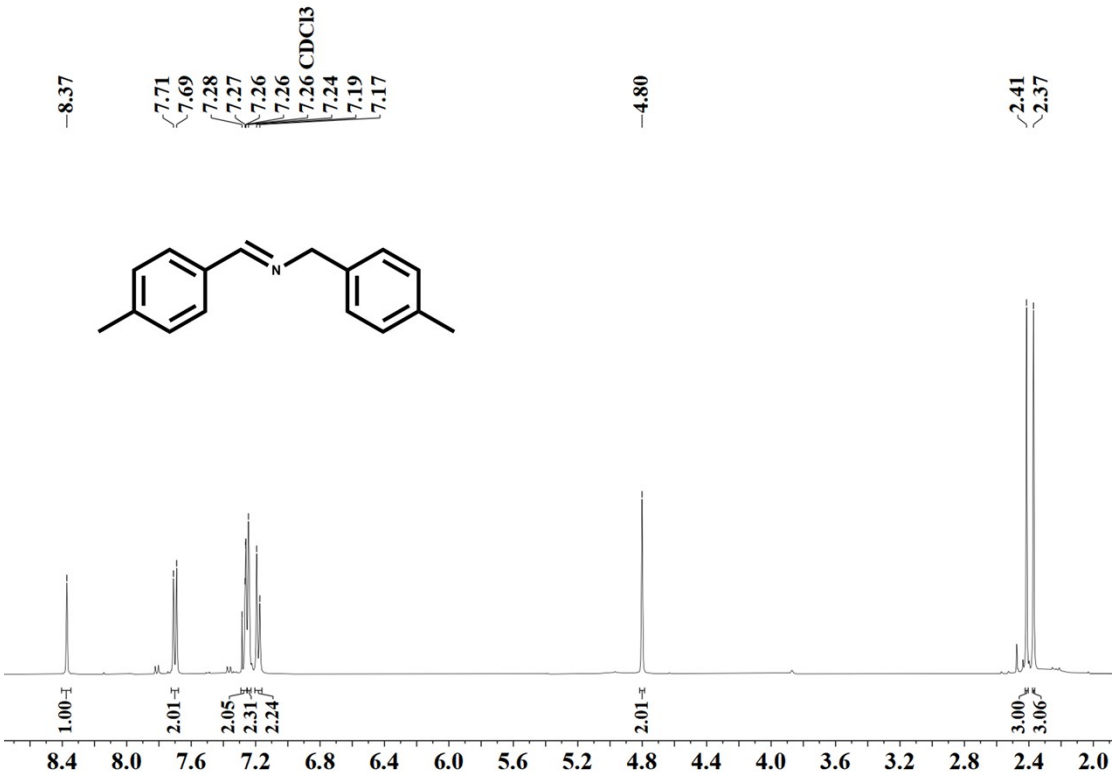
8.37
7.71
7.69
7.28
7.27
7.26
7.26
7.26 CDCl3
7.24
7.19
7.17
4.80
2.41
2.37
N
1.00
2.01
2.05
2.31
2.24
2.01
3.00
3.06
8.4
8.0
7.6
7.2
6.8
6.4
6.0
5.6
5.2
4.8
4.4
4.0
3.6
3.2
2.8
2.4
2.0

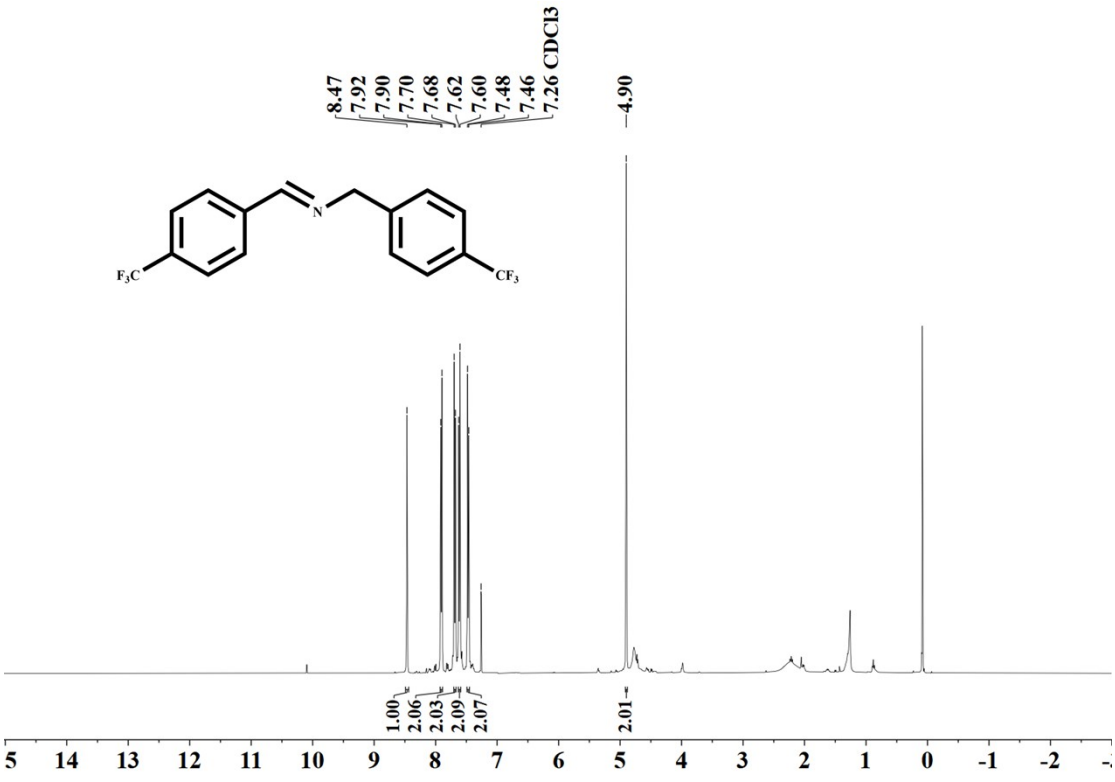
8.47
7.92
7.90
7.70
7.68
7.62
7.60
7.48
7.46
7.26 CDCl3
4.90
N
F3C
CF3
1.00
2.06
2.03
2.09
2.07
2.01
5
14
13
12
11
10
9
8
7
6
5
4
3
2
1
0
-1
-2

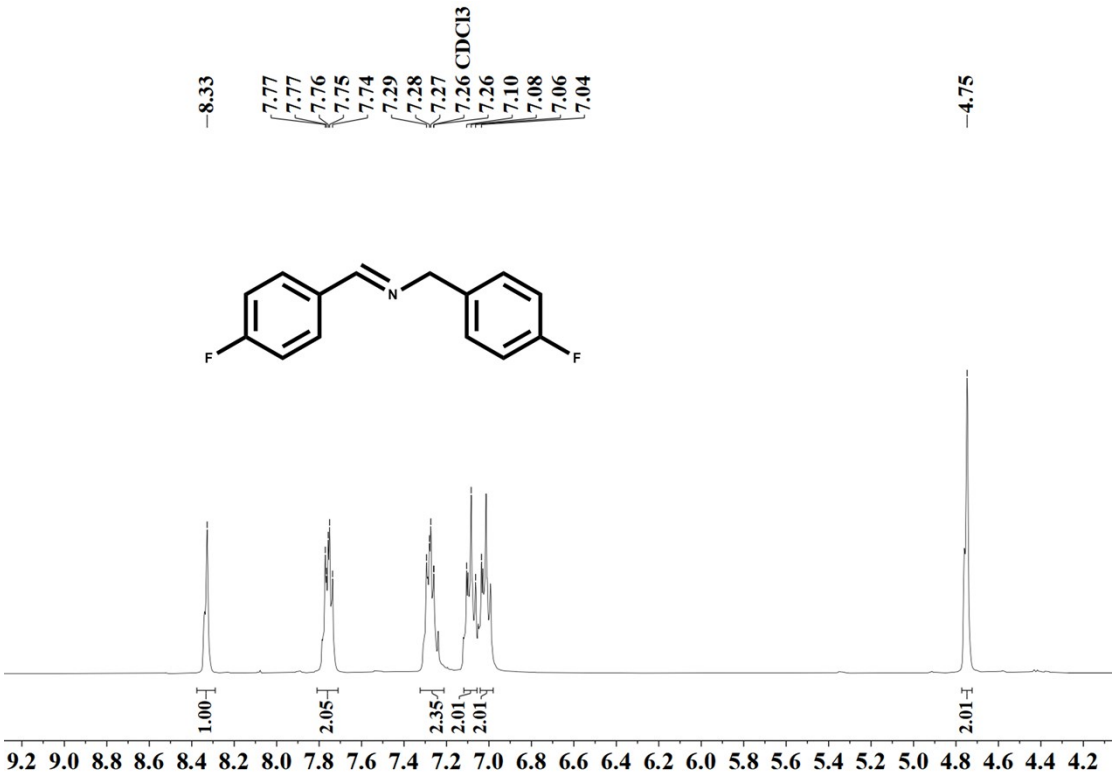
8.33
7.77
7.77
7.76
7.75
7.74
7.29
7.28
7.27
7.26 CDCl3
7.26
7.10
7.08
7.06
7.04
4.75
F
N
F
1.00
2.05
2.35
2.01
2.01
2.01
9.2 9.0 8.8 8.6 8.4 8.2 8.0 7.8 7.6 7.4 7.2 7.0 6.8 6.6 6.4 6.2 6.0 5.8 5.6 5.4 5.2 5.0 4.8 4.6 4.4 4.2

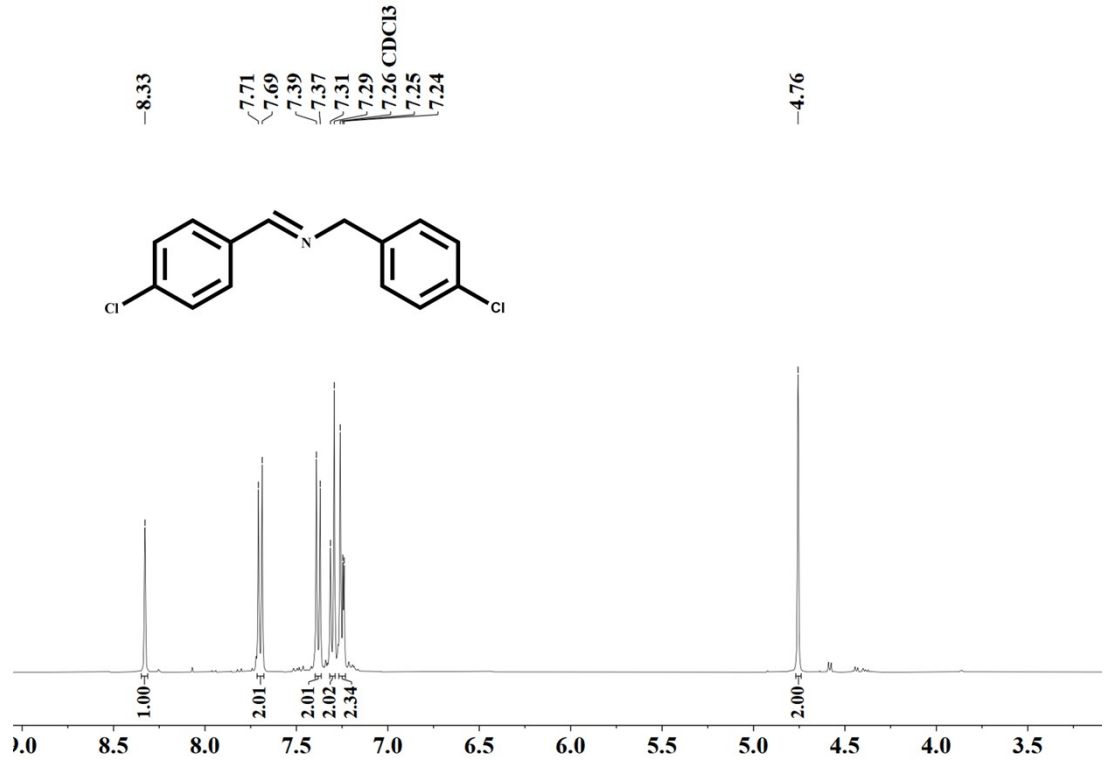
8.33
7.71
7.69
7.39
7.37
7.31
7.29
7.26 CDCl3
7.25
7.24
4.76
Cl
N
Cl
1.00
2.01
2.01
2.02
2.34
2.00
0.0 8.5 8.0 7.5 7.0 6.5 6.0 5.5 5.0 4.5 4.0 3.5

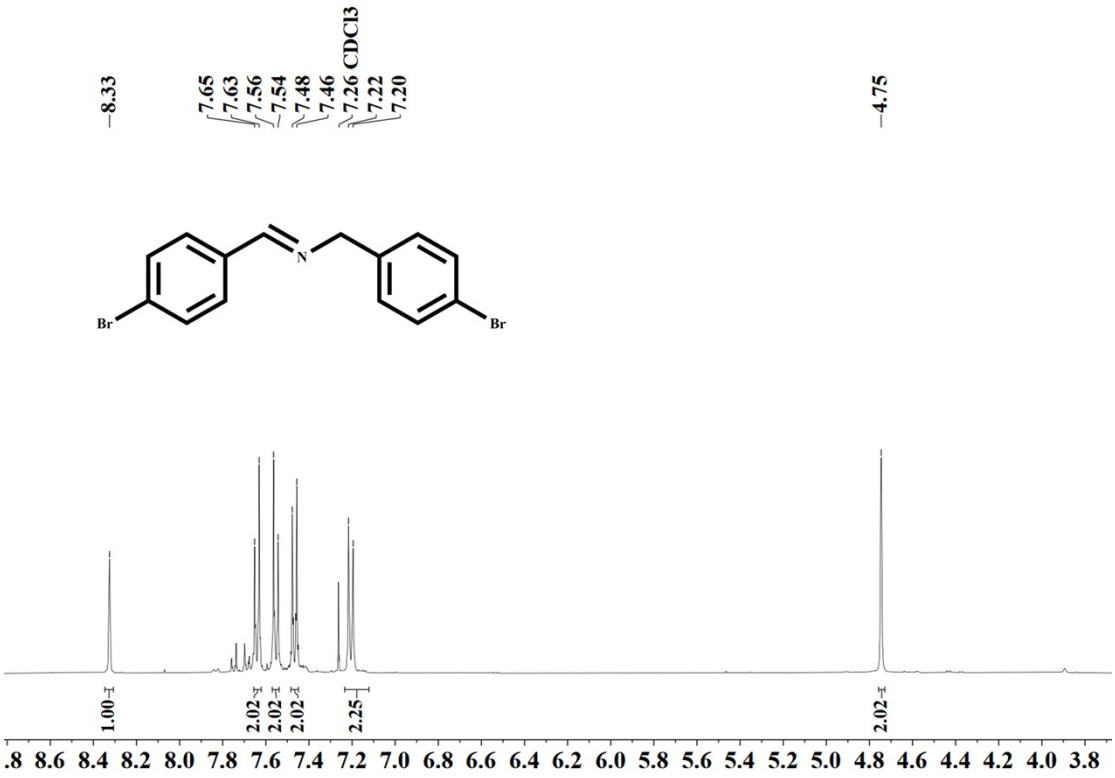
8.33
7.65
7.63
7.56
7.54
7.48
7.46
7.26 CDCl3
7.22
7.20
4.75
N
Br
Br
1.00
2.02
2.02
2.02
2.25
2.02
.8 8.6 8.4 8.2 8.0 7.8 7.6 7.4 7.2 7.0 6.8 6.6 6.4 6.2 6.0 5.8 5.6 5.4 5.2 5.0 4.8 4.6 4.4 4.2 4.0 3.8

Reference

1. Kresse, G.; Hafner, J. Ab initio molecular dynamics for liquid metals. *Phys. Rev. B*, 1993, **47**: 558-561.

2. Kresse G.; Hafner J. Ab initio molecular-dynamics simulation of the liquid-metal–amorphous-semiconductor transition in germanium. *Phys. Rev. B*, 1994, **49**: 14251-14269.

3. Kresse, G.; Furthmüller J. Efficiency of ab-initio total energy calculations for metals and semiconductors using a plane-wave basis set. *Comput. Mater. Sci*., 1996, **6**: 15-50.

4. Kresse, G.; Furthmüller, J.; Efficient iterative schemes for ab initio total-energy calculations using a plane-wave basis set. *Phys. Rev. B*., 1996, **54**, 11169-11186.

5. Blöchl, P. E. Projector augmented-wave method. *Phys. Rev. B*, 1994, **50**, 17953-17979.

6. Kresse, G.; Joubert, D. From ultrasoft pseudopotentials to the projector augmented-wave method. *Phys. Rev. B*, 1999, **59**, 1758-1775.

7. Perdew, J. P.; Burke, K.; Ernzerhof, M. Generalized gradient approximation made simple. *Phys. Rev. B*, 1996, **77**, 3865-3868.

8. Grimme, S. Density functional theory with London dispersion corrections. *Wires Comput. Mol. Sci*., 2011, **1**, 211-228.

9. Wang, V.; Xu, N.; Liu, J. C.; Tang, G.; Geng, W. T. VASPKIT: a user-

friendly interface facilitating high-throughput computing and analysis using VASP code. *Comput. Phys. Commun*., 2021, **267**, 108033.